

# Image De-noising on Strip Steel Surface Defect Using Improved Compressive Sensing Algorithm

Dongyan Cui<sup>1,2</sup>, Kewen Xia<sup>\*1</sup>, Jingzhong Hou<sup>1</sup>, and Ahmad Ali<sup>1</sup>

<sup>1</sup>School of Electronics Information Engineering, Hebei University of Technology  
Tianjin/China/Hebei University of Technology

<sup>2</sup>School of Information Engineering, North China University of Science and Technology  
Tangshan/China/North China University of Science and Technology

Corresponding author, e-mail: kwxia@hebut.edu.cn

## Abstract

De-noising for the strip steel surface defect image is conducive to the accurate detection of the strip steel surface defects. In order to filter the Gaussian noise and salt and pepper noise of strip steel surface defect images, an improved compressive sensing algorithm was applied to defect image de-noising in this paper. First, the improved Regularized Orthogonal Matching Pursuit algorithm was described. Then, three typical surface defects (scratch, scar, surface upwarping) images were selected as the experimental samples. Last, detailed experimental tests were carried out to the strip steel surface defect image de-noising. Through comparison and analysis of the test results, the Peak Signal to Noise Ratio value of the proposed algorithm is higher compared with other traditional de-noising algorithm, and the running time of the proposed algorithm is only 26.6% of that of traditional Orthogonal Matching Pursuit algorithms. Therefore, it has better de-noising effect and can meet the requirements of real-time image processing.

**Keyword:** compressive sensing, surface defects, image de-noising

*Copyright © 2017 Universitas Ahmad Dahlan. All rights reserved.*

## 1. Introduction

Image noise reduction is a classical problem in image processing which has over 50 years of research history [1, 2], and still is a hot topic. The strip steel surface defect images in the process of collection, acquisition and transmission will be polluted to some extent by visible or invisible noise, also due to the unstable light, camera vibration and other factors etc. Therefore, it is necessary to carry out the noise processing of the collected images.

A large number of studies have been carried out on the surface defect image de-noising at home. In 2008, Liu Weiwei, Yun Hui Yan et al of Northeastern University put forward an image de-noising method based on local similarity analysis and neighborhood noise evaluation [3]; In 2010, Bo Tang et al studied the rules of strip steel surface defects image de-noising based on wavelet threshold [4]; In 2012, Hao Xu of Wuhan University of Science and Technology proposed the method of surface defect of strip steel based on mathematical morphology, which could detect small defect edge under strong noise and own strong noise immunity [5].

From the above, the existing strip steel surface defect image de-noising methods mainly focused on the traditional filtering method. In the existing theory, the original signal is mostly projected to a certain transformation space, and the sparsity of the coefficient in the projection domain is as a fundamental basis. While the existence of noise affected the sparsity of signals in the transform space. So the optimization method is used to restore the signal, if only a single sparse constraint principle is used, it is difficult to accurately reconstruct the original signal. In this case, compressive sensing theory still may take other effective method of reconstructing. Numerous studies show that the reconstruction algorithm based on compression perception theory is applied in signal de-noising can achieve good effect [6]-[8]. Donoho [9]-[10], Candes [11]-[13], Romberg [11]-[13] and Tao [12]-[13] and other scientists initially put forward the concept of compressed sensing from sparse signal decomposition and approximation theory in 2004, followed by a large number

of relevant theoretical research. M.A.T. Figueiredo proposed the gradient projection for sparse reconstruction(GPSR)algorithm based on the L1 norm. The method obtained the good effect of denoising [14].

The compressed perception theory is introduced into the strip steel surface defect image preprocessing, which is rarely mentioned in the literature at home and abroad. Therefore, In this paper, the improved ROMP algorithm was applied to the strip steel surface defect image de-noising, which has better de-noising effect and shorter running time compared with traditional median filtering, wavelet threshold method and traditional compressed sensing algorithm.

## 2. Research Method

### 2.1. Description of weighted ROMP algorithm

Needell et al proposed the regularized orthogonal matching pursuit algorithm (ROMP) based on the orthogonal matching pursuit (OMP)[15]-[16]. All matrices satisfied the restricted isometry condition and all sparse signals can be reconstructed.

The algorithm was improved based on ROMP algorithm. The selection of atomic index set for the first time was using weighted correlation coefficient, not only considering the correlation coefficient of the current iteration, also considering the correlation coefficient of the last iteration, and expanding the selection scope of index value. Weighted formula is as shown in (1).

$$g^t = \alpha g + \beta g^{t-1} \text{ s.t. } g = A^T r^{t-1}, 0 < \alpha < 1, 0 < \beta < 1, \alpha + \beta = 1 \quad (1)$$

The pseudo code of algorithm is as follows.

Input:(1)measurement matrix  $y$ ,  $y \in R$ ;(2)  $M \times N$  dimensional sensing matrix  $A = \Phi\Psi$  ;(3) sparsity level  $K$  of the signal(the number of nonzero elements in  $x$ ).

Output  $N$  dimensional reconstructed signal(sparse approximation signal) $\hat{x} \in R^N$ .

Initialize  $r_0 = y$ ,  $\Lambda_0 = \phi$ ,  $A_0 = \phi$

Iteration

step(1)Calculate:  $g = \text{abs} [A^T r_{t-1}]$  (which is:  $\langle r_{t-1}, \alpha_j \rangle$ ,  $1 \leq j \leq N$ );

step (2)Obtain  $u = |g^t|$  according to formula (1),choose a set  $J$  of the  $K$  biggest or nonzero values, which corresponds to the column number of  $A$  and construct a set  $J$  ;

step (3)Regularize:  $|u_i| \leq 2 |u_j|$  for all  $i, j \in J_0$ , Among all subset  $J_0$ , choose  $J_0$  with the maximal energy  $\sum_j |u(j)|^2, j \in J_0$  ;

step (4) $\Lambda_t = \Lambda_{t-1} \cup J_0, A_t = A_{t-1} \cup \alpha_j$  (for all  $j \in J_0$ );

step(5) Calculate the least squares solution of  $y = A_t \theta_t$ :  $\hat{\theta}_t = \text{argmin}_{\theta_t} \|y - A_t \theta_t\| = (A_t \theta_t)^{-1} A_t^T y$ ;

step (6) Update residual:  $r_t = y - A_t \hat{\theta}_t = y - A_t (A_t^T A_t)^{-1} A_t^T y$

step (7)  $t = t + 1$ , if  $t \leq K$ , then return step (1), if  $t > K$  or  $\|\Lambda_t\|_0 \geq 2K$  ( $\|\Lambda_t\|_0$  represents the number of elements in the set or residua  $r_t = 0$ , then the iteration stop, and enter step (7);

step (8)  $\hat{\theta}_t$  has nonzero entries at  $\Lambda_t$  the value is respectively  $\hat{\theta}_t$  obtained from reconstruction

step (9) reconstructed the signal  $\hat{x} = \Psi \hat{\theta}$ .

### 2.2. De-noising Model Based On The Weighted Correlation ROMP Algorithm

Assuming that the received image signal is  $g(x, y)$ , which is contaminated by noise. The clean image is  $f(x, y)$ . The additive noise is  $n(x, y)$ . Then the additive noise model is  $g(x, y) = f(x, y) + n(x, y)$ . When the signal is disturbed by multiplicative noise, the model is expressed as in (2).

$$g(x, y) = f(x, y) (1 + n(x, y)) = f(x, y) + f(x, y) n(x, y) \quad (2)$$

Where, the output signal of the second term is the result of multiplying the noise, which is affected by  $f(x, y)$ . The bigger  $f(x, y)$ , the bigger the noise. According to the theory of compressive sensing, the following results can be obtained, as in (3).

$$g(x, y) = f(x, y) + n(x, y) = \phi \alpha \quad (3)$$

Where,  $\alpha$  is a sparse representation of the transformed image. In this way, we can recover the original image by estimating the sparse representation of the clean image so as to achieve the purpose of removing the noise.

The de-noising model based on the compressive sensing model is as in (4).

$$\alpha = \operatorname{argmin} \|\alpha\|_0, \text{ s.t. } \|\Phi\alpha - g\|_2^2 \leq T \quad (4)$$

### 3. Result and Analysis

Three kinds of strip steel defect images (scratch, scar, surface upwarping) are selected in this paper, and the noise type is Gaussian noise and salt and pepper noise.

#### 3.1. Simulation Experiment 1: Defect image de-noising polluted by Gaussian noise

Firstly, the effect of different transformation matrices on the image de-noising processing is studied. Sampling rate was 0.4, 0.5 and 0.4, respectively, as shown in Table 1.

Table 1. Comparison of different sampling rate and different transformation matrices

Defect type	M/N	FFT	FFT	DCT	DCT	DWT	DWT
		PSNR	time(s)	PSNR	time (s)	PSNR	time (s)
scratch	0.4	22.4548	3.451	20.6991	3.34	20.9255	0.98
	0.5	23.1268	4.891	20.6288	4.703	19.9260	1.282
	0.6	23.2428	6.493	20.6907	6.231	19.7568	1.843
scar	0.4	21.7367	3.541	18.7781	3.361	19.7284	0.94
	0.5	21.5880	4.932	19.2251	4.671	21.1243	1.361
	0.6	21.8828	6.392	19.9448	6.121	19.3047	1.841
surface upwarping	0.4	23.0123	3.641	19.9002	3.51	20.8668	1.21
	0.5	23.4251	5.323	19.8785	5.044	19.3613	1.469
	0.6	23.2042	6.924	20.1599	6.651	19.2570	1.9

From Table 1, we can get the comparison results of PSNR and run time under the DWT and FFT, DCT transform matrix. The PSNR value using DWT transformation matrix to process is higher than that of the DCT transform matrix, and is slightly lower than that of the FFT transform matrix. While the running time of the DWT transform matrix is much shorter than that of the other two. Obviously, the DWT transformation matrix can greatly shorten the running time, and it will not reduce the image quality. In this paper, the DWT transform matrix is applied in different compression sensing algorithms to process the strip surface defect image, so as to achieve the purpose of real-time processing.

Table 2 shows the de-noising results of three types of defects (scratch, scar, facial warping) under Gaussian noise using OMP, Cosamp, stomp and the proposed algorithm. The sampling rate is 0.5, The transformation matrix is the DWT matrix. The Gaussian noise mean is 0 and variance is 0.1, 0.01, 0.001 respectively, as shown in Table 2 below.

From the experimental data and experimental results, the PSNR value is higher than the OMP algorithm, Cosamp algorithm and StOMP algorithm using the proposed method to de-noise the strip steel surface defect image. Although the running time is slightly higher than that of the StOMP algorithm, but compared with the OMP algorithm and the Cosamp algorithm, the running time is greatly reduced, about 26.6% of the OMP algorithm and 41.7% of the Cosamp algorithm. Experiments show that, considering the de-noising effect and the running time, the performance of this algorithm to handle strip surface defect image Gaussian noise pollution is optimal. Type of experiment defects respectively are scratch, scar and surface upwarping. Gauss noise means is 0, the variance is 0.1, 0.02, 0.01, 0.005.  $3 \times 3$  templates is selected in mean filter and median filter for processing. Figure 1(a)-(g) to figure3(a)-(g) are respectively the results of three kinds of defects when the Gaussian noise mean is 0 and the variance is 0.01. Table 4 shows the PSNR values of three kinds of defects using various de-noising algorithms (Gaussian noise with mean 0

Table 2. Gaussian noise de-noising effect when the sampling rate is 0.5

Defect type	Gaussian Noise	OMP PSNR	OMP Time(s)	Cosamp PSNR	Cosamp Time(s)	StOMP PSNR	StOMP Time(s)	Proposed PSNR	Proposed Time(s)
scratch	0.1	15.0269	11.373	11.3264	8.1589	9.6994	1.995	26.7728	2.9952
	0.01	24.1047	11.546	17.9604	7.1916	18.7309	2.139	29.9563	3.0888
	0.001	33.4488	11.345	21.1458	7.3788	27.6014	2.124	33.6600	3.0576
scar	0.1	18.3338	11.152	11.4972	7.2696	9.7740	1.588	26.7509	2.9952
	0.01	24.0836	11.500	17.4030	7.1760	18.5289	1.907	29.2152	3.0420
	0.001	33.1111	11.729	19.9023	7.1760	27.2120	1.484	32.3062	3.1356
surface upwarping	0.1	15.1427	11.431	11.3537	7.2384	9.7414	0.8569	26.5816	3.1512
	0.01	23.7802	11.607	17.0315	7.1448	18.2017	0.3639	29.3068	2.9952
	0.001	32.5775	11.400	19.6132	7.0824	24.7782	0.1734	32.5256	3.0108

and variance 0.01). Figure 4 (a)-(c) are respectively the PSNR comparison curve of three kinds of defects noisy images obtained by using various de-noising algorithms.

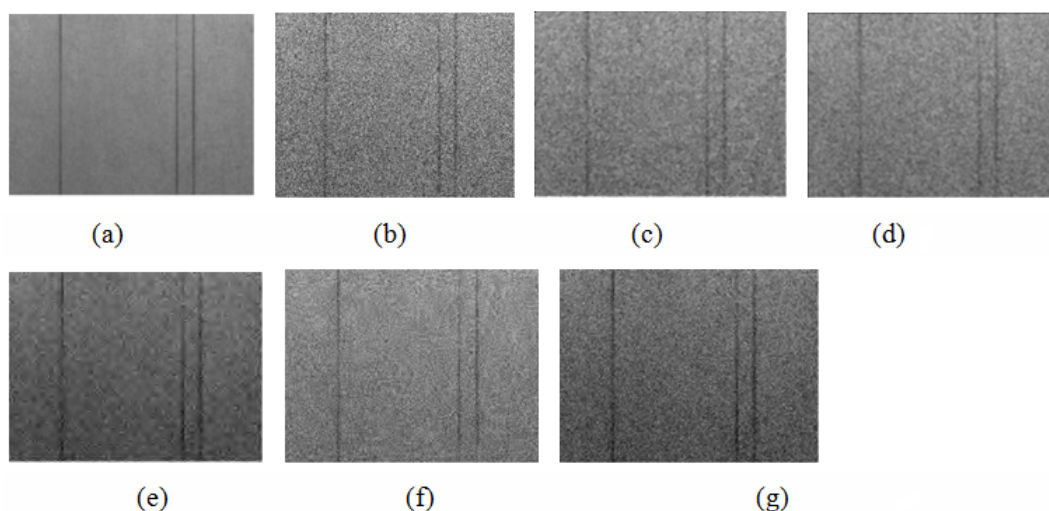


Figure 1. scratch(Gaussian noise with mean 0 and variance 0.01)(a) the original image of scratch (b) the image with Gaussian noise (c) Median filtering image (d) Mean filtering image (e) Wavelet de-noising image (f)CS de-noising image (g) de-noising image of the proposed algorithm

As shown in Table 3 and Figure 4, the PSNR values of the various algorithms are all decreased with the increasing of the noise intensity. Compared with other traditional de-noising methods, the proposed method in this paper has higher PSNR value, that is, the effect is better.

### 3.2. Simulation Experiment 2: Defect image de-noising polluted by salt and pepper noise

Type of defects are respectively scratch, scar and facial warping in the experiment. Salt and pepper noise intensity are 0.1, 0.01, 0.005, 0.001. 3\*3 templates is selected in mean filter and median filter for processing. Figure 5(a)-(g) to figure 7(a)-(g) are respectively the results of three kinds of defects de-noising images. Table 4 shows the PSNR values of three kinds of defects using various de-noising algorithms (Salt and pepper noise intensity is 0.1). Figure 8 (a)-(c) are respectively the PSNR comparison curve of three kinds of defects noisy images obtained by using various de-noising algorithms.

As shown in Table 4 and Figure 8, the PSNR values of the various algorithms are all decreased with the increasing of the noise intensity. The median filtering method is very effective for the de-noising of salt and pepper noise. Compared with other traditional de-noising methods,

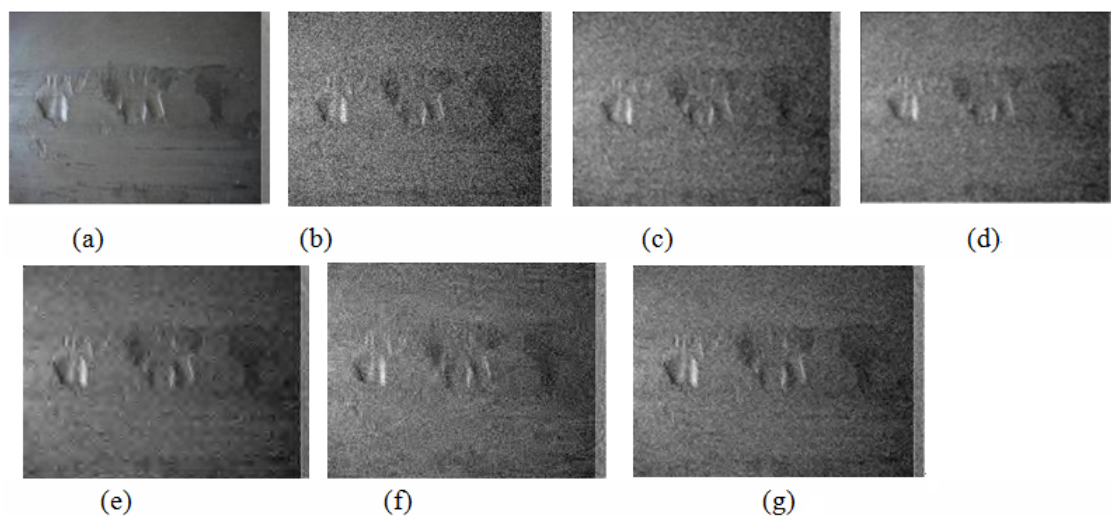


Figure 2. scar(Gaussian noise with mean 0 and variance 0.01)(a) the original image of scar (b) the image with Gaussian noise (c) Median filtering image (d) Mean filtering image(e) Wavelet de-noising image (f)CS de-noising image (g) de-noising image of the proposed algorithm

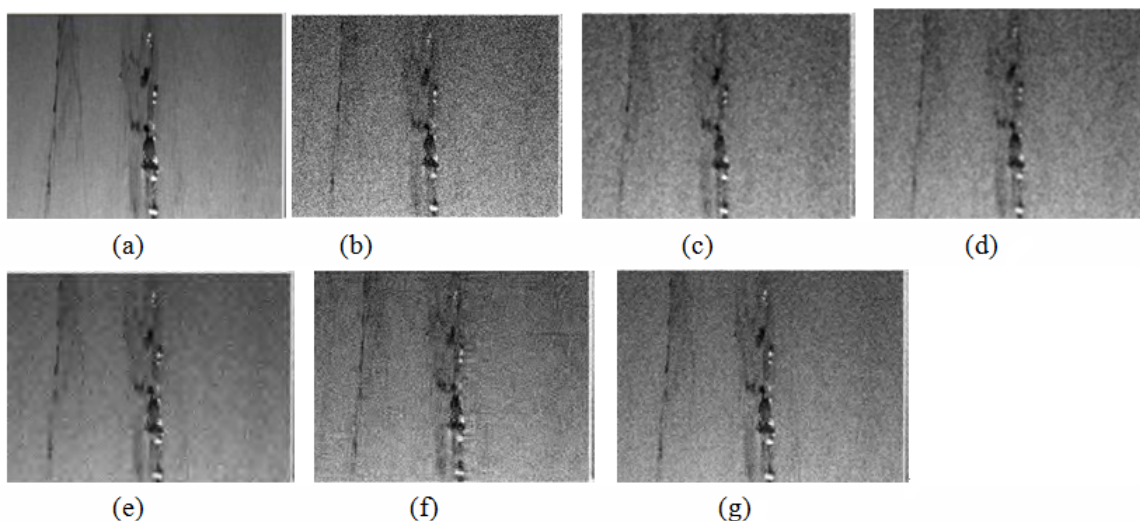


Figure 3. surface upwarping(Gaussian noise with mean 0 and variance 0.01)(a) the original image of surface upwarping (b) the image with Gaussian noise (c) Median filtering image (d) Mean filtering image(e) Wavelet de-noising image (f)CS de-noising image (g) de-noising image of the proposed algorithm

the proposed method in this paper has higher PSNR value, that is, the effect is better.

#### 4. Conclusion

For cold-rolling complex environment, and its image in the acquisition, acquisition, transfer process will be polluted by visible or invisible noise, we focus on de-noising method based on the improved compressive sensing algorithm. The conclusions are as follows:

- (1) In the compressive sensing algorithm, the image quality and running time are affected by different transformation matrix. Considering the two, the DWT transform matrix is the best.
- (2) Under the same noise intensity, the proposed algorithm has a little difference on the

Table 3. The de-noising effect of various algorithms with different intensity Gaussian noise

Defect	Noise	PSNR0	Median filter	Mean filter	wavelet	CS-OMP	proposed
scratch	0.1	12.7296	17.5589	19.0174	24.1869	15.0130	26.7728
	0.02	18.6791	24.0706	23.2626	24.0905	20.9537	26.8191
	0.01	21.5005	26.7408	24.3423	24.0711	23.8867	29.9563
	0.005	24.2483	29.2443	25.2858	24.0755	26.7766	32.6602
scar	0.1	12.9701	17.4094	18.8318	23.8928	15.1302	26.7509
	0.02	18.7187	23.8616	22.7633	23.8432	20.9413	26.9985
	0.01	21.5438	26.3853	23.7873	23.8198	23.6766	29.2152
	0.005	24.1825	28.8335	24.7421	23.8063	26.5264	31.2532
surface upwarping	0.1	12.8528	17.1803	18.6847	23.6883	15.0231	26.5816
	0.02	18.3413	23.0985	22.4577	23.6199	20.8064	26.8462
	0.01	20.8621	25.2768	23.5022	23.6304	23.4988	29.3068
	0.005	22.9852	26.9534	24.0940	23.5888	26.1000	32.6708

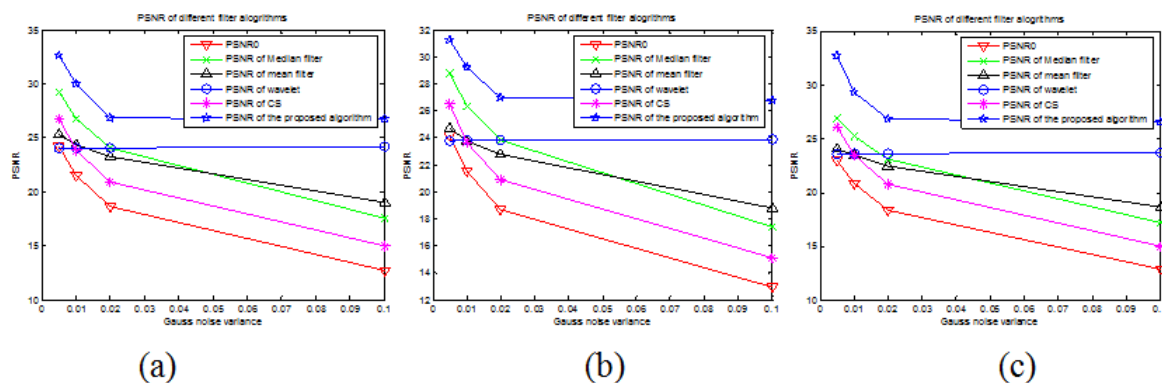


Figure 4. the PSNR comparison curve obtained by using various de-noising algorithms (a) The PSNR curve of scratch image (b) The PSNR curve of scar image (c) The PSNR curve of surface upwarping image

de-noising effect for different kinds of defects.

(3) Compared with the traditional algorithm such as median filtering, mean filtering, wavelet de-noising and conventional compression sensing method, the proposed method has better de-noising effect.

### Acknowledgement

This work was supported by the National Natural Science Foundation of China (No. 51208168), and Hebei Province Natural Science Foundation (No. E2016202341).

### References

- [1] Zhang Ye, Jia Meng, "Underground Image Denoising" *TELKOMNIKA Indonesian Journal of Electrical Engineering*, vol. 12(6), pp.4438-4443, 2014.
- [2] WANG Jianwei, "A Noise Removal Algorithm of Color Image" *TELKOMNIKA Indonesian Journal of Electrical Engineering*, vol. 12(1), pp.565-574, 2014.
- [3] Weiwei Liu, Yan Yun-hui, Sun Hong-wei et al., "Impulse noise reduction in surface defect of steel strip images based on neighborhood evaluation," *Chinese Journal of Science Instrument*, Vols 29, pp. 1846-1850, 2008.
- [4] Bo Tang, Kong Jian-yi, Wang Xing-dong et al., "Wavelet threshold denoising for steel strip surface defect image," *Journal of Wuhan University of Science and Technology*, Vols 33, pp.

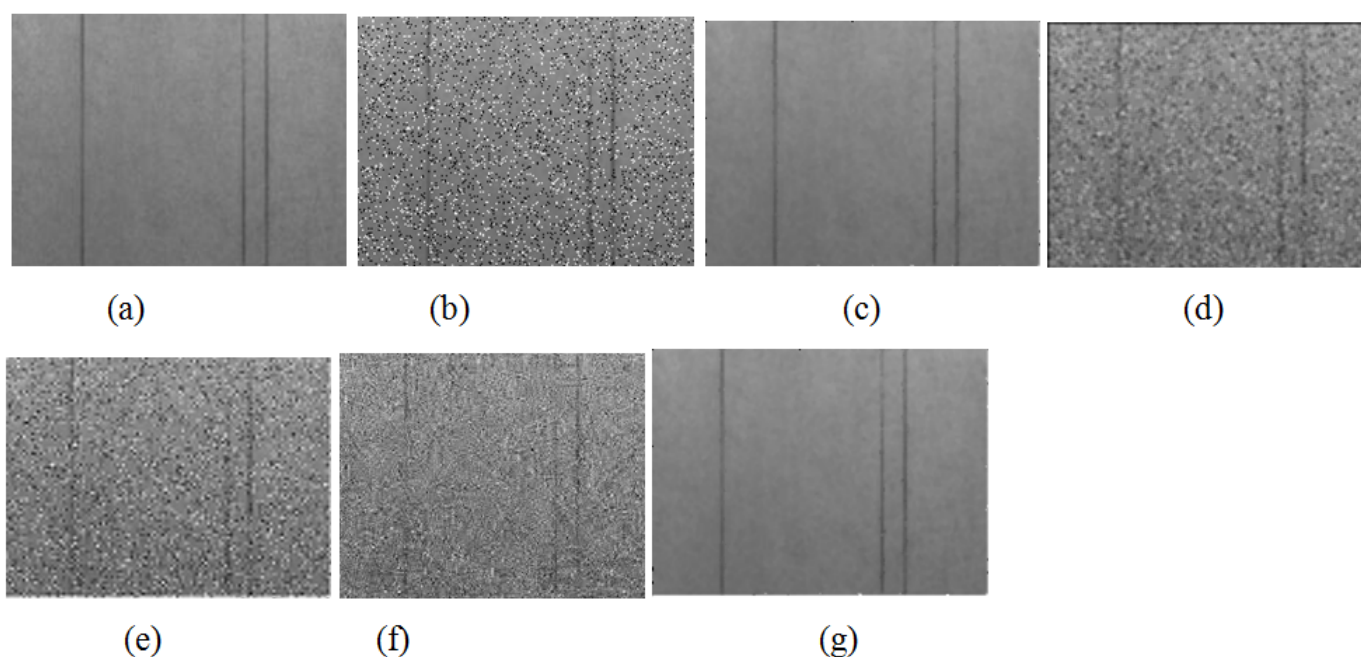


Figure 5. scratch(Salt and pepper noise intensity is 0.1)(a) the original image of scratch (b) the image with Gaussian noise (c) Median filtering image (d) Mean filtering image (e) Wavelet de-noising image (f)CS de-noising image (g) de-noising image of the proposed algorithm

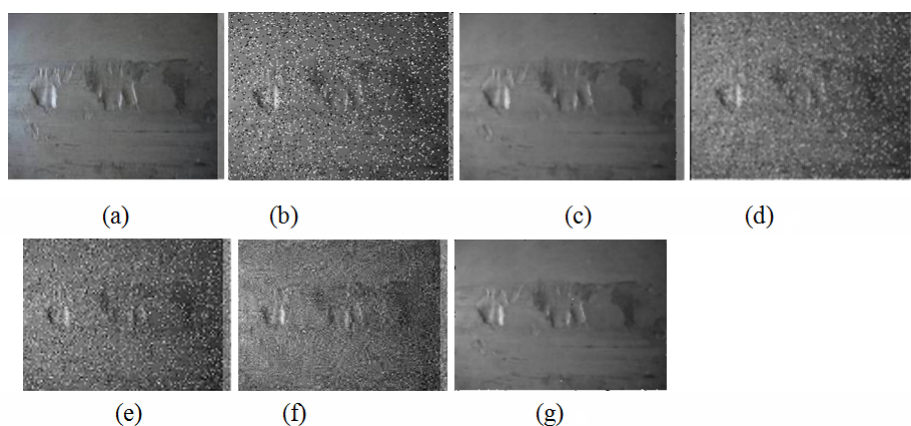


Figure 6. scar(Salt and pepper noise intensity is 0.1)(a) the original image of scar (b) the image with Gaussian noise (c) Median filtering image (d) Mean filtering image (e) Wavelet de-noising image (f)CS de-noising image (g) de-noising image of the proposed algorithm

38-42,2010.

- [5] Hao Xu, "Image processing and identification of strip steel surface defects based on machine vision," *Thesis for master's degree of Wu Han University of science and technology*,2012.
- [6] Amin Tavakoli, Ali Pourmohammad, "Image Denoising Based on Compressed Sensing," *International Journal of Computer Theory and Engineering*, Vols 4, pp. 266-269,2012.
- [7] Shunli Zhang, "Compressed Sensing Method Application in Image Denoising," *International Journal of Signal Processing, Image Processing and Pattern Recognition*, Vols 8, pp. 203-212,2015.
- [8] M. T. Alonso, P. L. Dekker and J. J. Mallorqui, "A Novel Strategy for Radar Imaging Based

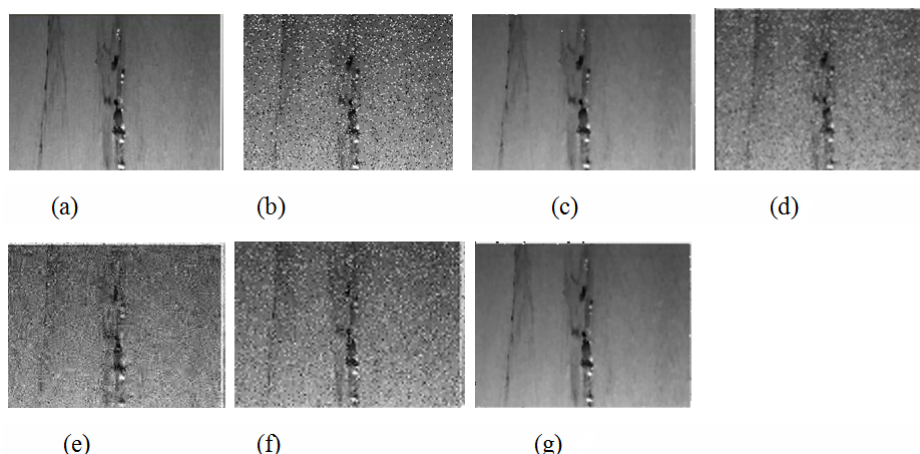


Figure 7. surface upwarping(Salt and pepper noise intensity is 0.1)(a) the original image of surface upwarping (b) the image with Gaussian noise (c) Median filtering image (d) Mean filtering image(e) Wavelet de-noising image (f)CS de-noising image (g) de-noising image of the proposed algorithm

Table 4. The de-noising effect of various algorithms with different intensity Salt and pepper noise

Defect	Noise	PSNR0	Median	Mean	wavelet	CS-OMP	Proposed
scratch	0.1	17.5990	31.5663	22.3715	23.4050	20.1083	31.5687
	0.01	26.7632	36.4494	26.3376	30.6689	32.4924	37.3122
	0.005	28.6169	36.4548	26.7347	33.5300	35.9337	42.4640
	0.001	32.2959	36.4613	26.9791	37.1267	41.6660	48.3173
scar	0.1	17.3623	29.7687	21.9811	22.9747	19.7776	30.1205
	0.01	26.5068	34.8033	25.2883	29.3508	30.9695	36.5890
	0.005	28.4849	34.8155	25.6405	31.6003	34.4295	40.7194
	0.001	32.0367	34.8203	25.8779	35.0911	38.5237	45.1762
surface upwarping	0.1	17.0655	28.1653	21.9634	23.1624	19.8053	29.2302
	0.01	24.3441	29.7292	24.5819	28.2800	30.6486	34.7397
	0.005	25.7489	29.7268	24.8582	30.2394	32.7035	38.1562
	0.001	26.9719	29.7334	25.0317	32.4196	36.0263	42.2687

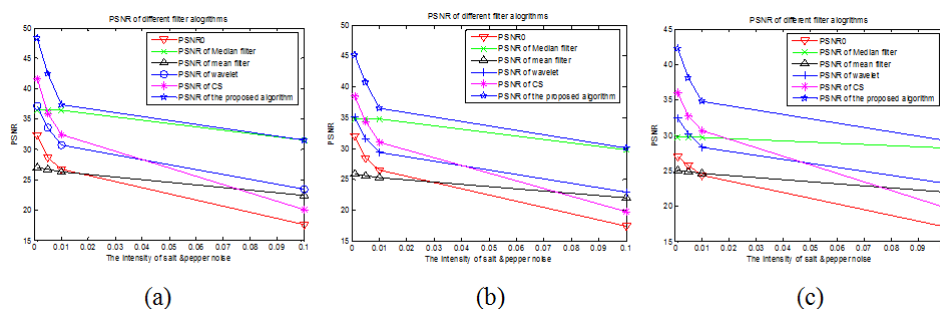


Figure 8. the PSNR comparison curve obtained by using various de-noising algorithms(a)The PSNR curve of scratch image (b) The PSNR curve of scar image (c) The PSNR curve of facial warping image

on Compressive Sensing,” *IEEE Trans. Geoscience and Remote Sensing*, Vols 48, pp. 4285-4295, 2010.

[9] D Donoho, ”Compressed sensing,” *IEEE Trans, on Information Theory*, Vols 52, pp. 1289-



- 1306,2006.
- [10] D Donoho, Y Tsaig, "Extensions of compressed sensing," *Signal Processing* , Vols 86, pp. 533-548,2006.
- [11] E. Candes , J. Romberg, "Sparsity and incoherence in compressive sampling," *Inverse Prob* , Vols 23, pp. 969-985,2007.
- [12] E. Candes, J. Romberg, T. Tao, "Robust uncertainty principles: Exact signal reconstruction from highly incomplete frequency information," *IEEE Trans. Inform. Theory* , Vols 52, pp. 489-509,2006.
- [13] E. Candes, J. Romberg, T. Tao, "Stable signal recovery from incomplete and inaccurate measurements," *Comm. Pure Appl. Math* , Vols 58, pp. 1207-1223,2006.
- [14] Figueiredo M A T , Nowak R D, Wright S J, "Gradient projection for sparse reconstruction: Application to compressed sensing and other inverse problems," *Journal of Selected Topics in Signal Processing: Special Issue on Convex Optimization Methods for Signal Processing* , Vols 194, pp. 586-598,2007.
- [15] Needell D, Vershynin R, "Signal recovery from incomplete and inaccurate measurements via regularized orthogonal matching pursuit," *IEEE Journal on Selected Topics in Signal Processing* , Vols 4, pp. 310-316,2010.
- [16] Zhenzhen Yang, Yang Zhen, Sun Linhui, "A Survey on Orthogonal Matching pursuit Type Algorithms for Signal Compression and Reconstruction," *Journal of Signal Processing* , Vols 29, pp. 486-496,2013.